*Progress In Electromagnetics Research, Vol. 147, 141–151, 2014*

# Super Resolution Laser Radar with Blinking Atmospheric Particles — Application to Interacting Flying Insects

**Mikkel Brydegaard[1, 2, 3, 4, *], Alem Gebru[2], and Sune Svanberg[1, 5]**

(*Invited Paper*)

**Abstract**—Assessment of biodiversity of pollinators on the landscape scale or estimation of fluxes of disease-transmitting biting midges constitutes a major technical challenge today. We have developed a laser-radar system for field entomology based on the so called Scheimpflug principle and a continuous-wave laser. The sample-rate of this method is unconstrained by the round-trip time of the light, and the method allows assessment of the fast oscillatory insect wing-beats and harmonics over kilometers range, e.g., for species identification and relating abundances to the topography. Whereas range resolution in conventional lidars is limited by the pulse duration, systems of the Scheimpflug type are limited by the diffraction of the telescopes. However, in the case of sparse occurrence of the atmospheric insects, where the optical cross-section oscillates, estimation of the range and spacing between individuals with a precision beyond the diffraction limit is now demonstrated. This enables studies of insect interaction processes *in-situ*.

## 1. REMOTE OPTICAL *IN-SITU* INSECT MONITORING

Although tiny in size, the massive number of insects makes them play a key role in most eco-systems around the globe. While the Western world experiences significant economic losses in agriculture due to lack of biodiversity and the colony collapse disorder of pollinators [1], disease vectors and pests are feared and, to a great extent, blamed for stagnating the development in tropical parts of the world.

Whereas birds can be ring marked or tracked via GPS or sun loggers, only the very largest and least abundant insects can be equipped with electronic tags [2, 3]. While research in the area of radar entomology has been conducted over several decades and numerous interesting applications have been described [4], laser radar (light detection and ranging; lidar) systems in the optical regime have the potential of achieving a far better sensitivity and address and classify even the tiniest insects, simply because most insects are much smaller than the wavelengths of microwaves used in radars but larger than the wavelengths of light. Further, optical off-the-shelf components allow spectral- and polarimetric target classification, providing molecular as well as microstructure information [5, 6]. Along these lines our group has previously demonstrated lidar remote detection of insects labeled with fluorescent powders, e.g., for assessing dispersal rates on a landscape scale [7, 8].

Today a major limitation in ecological entomology is that insect abundance assessment is based on sweep nets, light-, pheromone- or $CO_2$-traps. Placing and emptying the traps are tedious operations and constitute a major effort, and the results are known to be biased with respect to the species, sexes and age groups caught. Although trapping allows precise studies with microscopes, mass spectrometry

*Received 10 October 2014, Accepted 5 November 2014, Scheduled 10 November 2014*
* Corresponding author: Mikkel Brydegaard (mikkel.brydegaard@fysik.lth.se).
[1] Lund Laser Centre, Department of Physics, Lund University, P. O. Box 118, SE-221 00 Lund, Sweden. [2] Laser Research Institute, Department of Physics, University of Stellenbosch, Private Bag X1, 7602 Matieland, South Africa. [3] Centre for Animal Movement, Department of Biology, Lund University, Sölvegatan 37, SE-223 62 Lund, Sweden. [4] Norsk Elektro Optikk A/S, Prost Stabels vei 22, N-2019 Skedsmokorset, Norway. [5] Center of Optical and Electromagnetic Research, South China Normal University, Guangzhou 510006, China.

or genetics, online optical monitoring allows quantitative measures in terms of individuals per cubic meter per hour. A particularly simple and powerful approach to optical monitoring of insects is to direct a telescope towards a remote very black cavity [6]. When a sun-lit insect flies into the telescope field of view (FOV) the scattered light is observed on a close to zero background. Oscillations due to the wing-beats are observed using a fast broad-band optical detector, and the body scatter, the fundamental frequency, as well as several overtones, which contain a lot of characteristic information, can be recorded. Data of this kind from an InGaAs (0.8–1.7 μm) quadrant photodiode are shown in Fig. 1.

The instant optical monitoring allows precise activity correlation with environmental factors such as temperature and wind [6]. Furthermore, time-lag correlation analyses on the millisecond timescale between the occurrences of different insects occupying the probed air-volume reveal the interaction strength and kinetics between insect types [6]. A common observation is, for instance, that the likelihood of observing, e.g., a large predating dragonfly in a confined air-volume, significantly increases when that same air-volume was occupied by a prey in the previous milliseconds. Interaction mechanisms include predation, mating or territorial behavior, and the quantitative assessment would not only satiate our curiosity but could also be applied to identify matched predators, e.g., for suppressing invasive agricultural pests or reduce malaria spread.

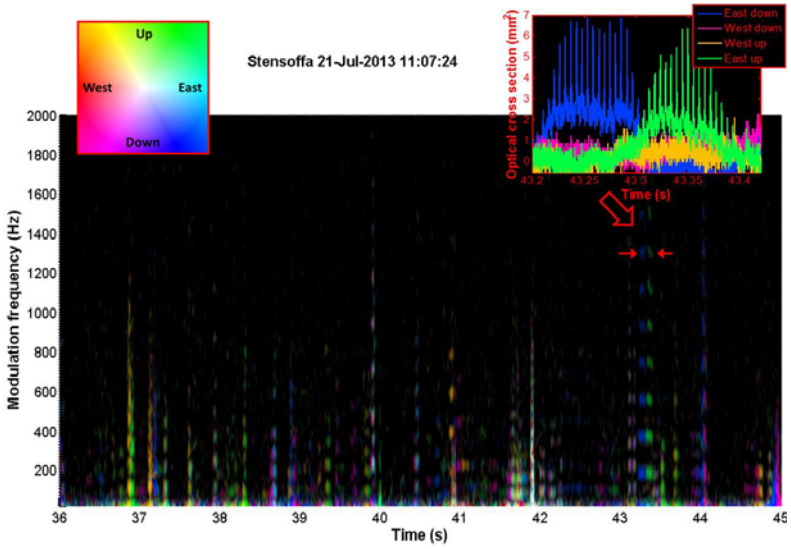


**Figure 1.** A representative fraction of quadrant dark-field observations at the Stensoffa biological field station, Sweden. From the oscillatory events read out by the detector segments, the frequency content (vertical scale) is calcultated by sliding Fourier transformation and is displayed with color coding. Approximately 10 $m^3$ of air is monitored, distributed over a 200 m path, yielding in the order of $10^4$ insect observation per hour. The distance is not determined by this line-of-sight method, but the temporal color change of each event indicates flight direction as discernable from the quadrant detector. As an example the oscillating detector element signals with color change from blue to green identifies an ascending individual at $t = 43.3$ s.

Apart from the close co-occurrence in time and space, insect interaction can additionally be confirmed by the flight direction of the interacting individuals. The flight heading can be revealed when using a quadrant detector and displaying the readout from the individual detector segments with color coding. (See Fig. 1). Aerial insect interaction is a tremendous technological challenge to study [9], and has so far mainly been accomplished in laboratory settings, where the insect behavior is known to differ considerably from that *in-situ*. Conventional lidars would generally not be able to resolve interacting atmospheric fauna separated by a few milliseconds in time and few centimeters in space. Here we present a diffraction unlimited method capable of doing so.

## 2. CLASSIFICATION AND INFORMATION IN OSCILLATORY PARTICLES

Blinking and oscillatory particles appear naturally in a number of situations ranging from molecules with switchable dark and fluorescent photo states, to stars with oscillating seismic modes in the μHz regime [10]. For the oscillatory property to be accessible the constellation of the particles either has to be sparse to an extent of single particle detection, such as in dilute single blinking molecule detection, or stars on the night sky, e.g., in astro-seismology — or coherent in phase, such as in the case of magnetic resonant imaging triggered by an alternating magnetic field. In entomology, the acquisition of the detailed modulation power spectrum from light scattered from insects has been demonstrated for species and gender recognition in laboratory settings [11, 12]. Corresponding modulation spectra can be retrieved remotely by a CW laser radar system, as demonstrated in Fig. 2, or by dark-field methods, as shown in Fig. 1, given that sample rates of at least several kHz are utilized.

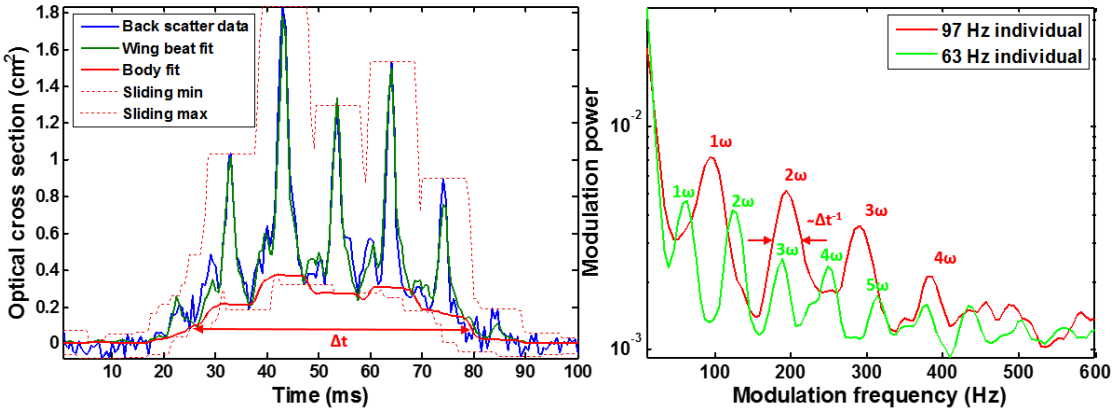


**Figure 2.** Examples of retrieved backscatter time series modulation spectra. Fig. 2(a). With a kHz rate sampling lidar, constituents of the atmospheric fauna cause rapid bursts in the air volume scatter coefficient. Here an example of an insect monitored several hundred meters away with a near-infrared beam at 808 nm wavelength is shown. The events can be parameterized with regression by a discrete sum of harmonics (green curve) weighted by the non-oscillatory insect body contribution (red curve). Fig. 2(b). Temporal modulation signature for two different insects at 75–85 m range, observed with a CW laser radar system operating at 808 nm. A low frequency body contribution is seen, as well as a fundamental frequency and various harmonics ($1\omega$, $2\omega$ etc.). The strengths of odd and even overtones are described by spherical functions of the physiological body orientation angles. $\Delta$t denotes the transition time through the probe volume.

Lidar backscattering from atmospheric fauna constituents is measured in terms of optical cross sections, in units of, e.g., square centimeters. The constituents appear as fast pulse bursts in the lidar data (See Fig. 2(a)). The signal bursts have an offset corresponding to the body size projection and an oscillatory part with an amplitude corresponding to the wing cross section.

The oscillatory waveform from glittering insects can contain several rapid superimposed spikes, corresponding to the specular reflectance conditions for the wings during the wing beat cycle. As a consequence of this, we have been able to observe up to eighteen overtones, each with specific amplitudes and phases. Entomologists are aware of a number of species where wings of young individuals displays glittering properties. This is associated with the metamorphosis when insectsemerge from their pupas and wings must be flexible. In the following days the wings harden and the optical properties become matte, see e.g., [13]. In bio-photonics, glittering and matte properties are associated with the refractive index and the de-polarization ratio. So far optical insect age assessment has been pursued in laboratory settings [14, 15], but in principle assessment could be achieved remotely.

Once the fundamental frequency is determined, the bursts (blue signal in Fig. 2(a)) can be smoothed by a low-pass filter with a corresponding bandwidth in order to extinguishing the fundamental frequency.

The burst can then be parameterized accurately by a regression with a discrete sum of harmonics (green signal Fig. 2(a)) weighted by the body size projection (red signal in Fig. 2(a)). The implication of such weighting is that the oscillatory base functions becomes zero when a body is not present in the probe volume.

The scattering cross sections of the off-set, the fundamental frequency and each harmonics are spherical functions in the physiological coordinate system, and can be expressed as a linear combination of a set of spherical harmonics or associated Legendre polynomials. Generally, the body cross section and the even harmonics are large in the sagittal plane, while the fundamental and odd harmonics are large in the transversal plane. In the frontal plane body scatter, the fundamental and odd overtones are large. The relation between overtone strengths and lidar interception angles of the insect observations is described in details elsewhere [16]. In the same work several symmetries are discovered and the formulation of absolute cross section look up tables for atmospheric fauna is proposed. From the angular dependence of the harmonics, it can be understood that the body orientation in space can be accessed via a kHz sampling lidar, in particular when symmetry is broken with quadrant detection such as in Fig. 1.

We have earlier shown how detailed wing beat waveforms in several spectral bands can yield remote microscopic information in bird feathers [5]. Equivalently, remote nanoscopy may be conducted of insect wing membranes using multi-band lidars, which, so far, have been developed for conventional aerosol particle characterization [17, 18]. The membrane thickness is known to be species specific [19]. As an example of useful data retrievable by optical means we present push-broom hyper-spectral images (VNIR and SWIR Hyspex camera, Norsk Elektro Optikk) of a wasp with selected examples of coherent and incoherent scatter spectra from both body and wings (See Fig. 3). Illumination was arranged in 45° with respect to the field of view. Similar findings are found for a large selection of other insect classes [20].

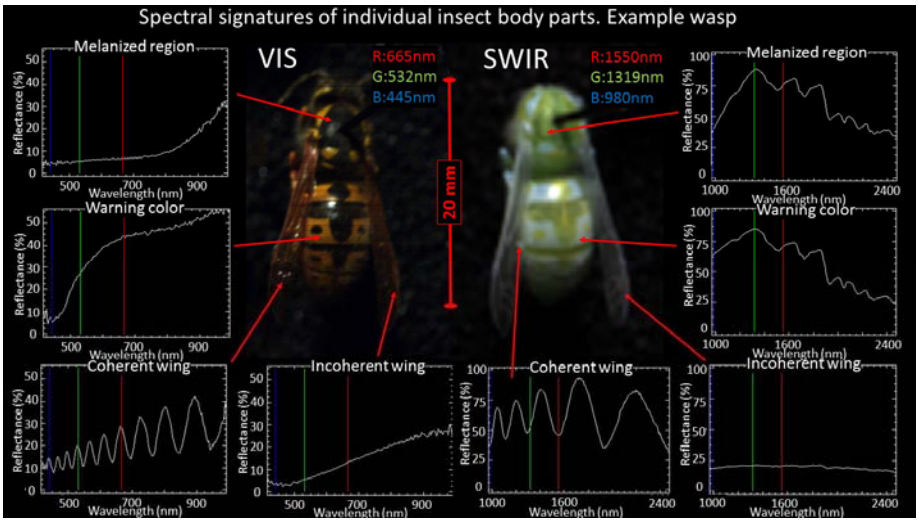


**Figure 3.** An example of a wasp seen at common laser wavelengths with hyperspectral imaging. Left: visible (VIS) true color. Right: Short-Wave-Infrared (SWIR) false color. In this case the spectral signature from the non-oscillatory body contributions due mostly to melanin, and the spectrum from a characteristic yellow warning spots are shown. The wings have two contributions; one diffuse (incoherent) and one specular (coherent). The diffuse scatter accounts for the fundamental beat frequency and lower harmonics, the contribution steadily increases throughout the visible spectrum peaking in the SWIR. The specular reflex accounts for spikes in the time domain or the higher harmonics in the frequency domain. The spectral signature of the specular reflex is a modulation from the Fabry-Perót-like interference in the membrane with a given free-spectralrange. The periodicity, amplitude and phase are directly related to the thickness of the membrane and the refractive index by the equation in, e.g., [21]. The thickness has been shown to be species specific [19], and the refractive index isknown to be associated with the age forseveral insects as discussed above.

## 3. SCHEIMPFLUG LIDAR

After we have developed these introductory examples of new optical techniques, we will now describe the main finding of the present work — sub-natural (super) resolution imaging of insects with a novel CW lidar design. Unaware of laser technology to come, in the year 1904 Captain Theodor Scheimpflug developed and patented a method in aerial photography, in which focus could be achieved consistently for perspective planes imaged at skew angles. In our present context, this implies that a laser beam transmitted out into the atmosphere can be imaged onto a straight line such as a tilted high-speed line-scan camera, in a way such that the pixel footprints coincide exactly with the illuminated air volumes (See Fig. 4). In other words, infinite focal depth can be achieved without closing the aperture. A number of angles, distances and equations can be postulated for achieving the Scheimpflug condition [22], but the solution is conveniently found by imposing three conditions: 1) the plane of the CCD, the receiving lens and the transmitted beam coincide in the same point, 2) the ray impinging at the outermost pixel, representing infinity, through the center of the receiving lens is parallel to the transmitted beam, 3) the distance from the receiving lens to the infinity pixel is equal to the focal length of the receiving telescope. We meet these conditions with two 102 mm diameter, 500 mm focal length refracting telescopes (StarTravel, SkyWatcher), a CCD tilt angle ($\beta$ in Fig. 4) of 40° and a transmitter and receiver separation of 602 mm. The parallelism of transmitter and receiver ($\alpha$ in Fig. 4) was 1.6°. We used a 3.2 W, 808 nm, $1 \times 100$ µm, CW laser diode (O-like Lasers). We employ a line-scan camera (Spyder3, DALSA Teledyne Inc), preceded by a Scott 4" RG780 long-pass colored-glass filter and a 2" 810 nm 10 nm FWHM, OD 4, band-pass filter (Knight Optical). The band-pass could potentially be as narrow as 1 nm FWHM on such F/5 telescopes.

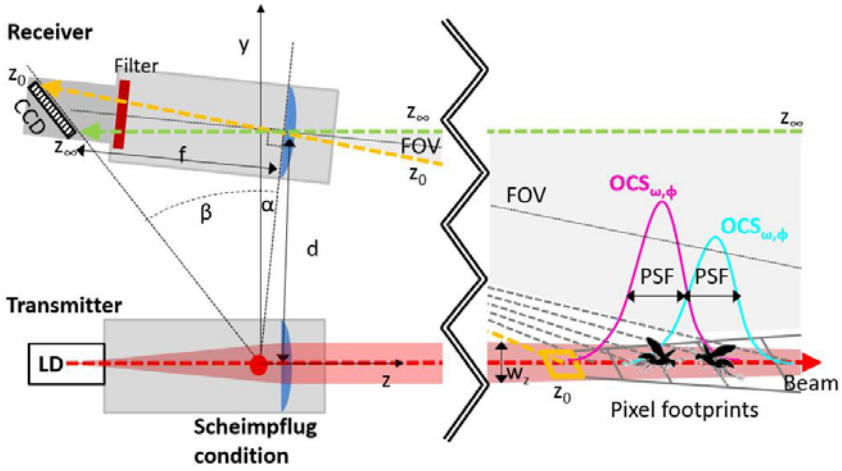


**Figure 4.** Through the Scheimpflug principle, where the imager plane and the lens plane coincide with the object plane, which in lidar is equivalent to the lidar beam, infinite focal depth can be achieved without closing the aperture. In such a triangulation configuration, the different ranges are imaged onto different positions of a detector array, and the range resolution is constraining by the diffraction limit of the receiver as well as the beam width. Small sparse constituents of the atmospheric fauna would produce echoes with resemblance of the point spread function. The blinking property, however, allows the discrimination of closely occurring constituents.

The beam is terminated on a remote black cardboard target with known reflectance, in the case presented here at a range of 1.8 km. To achieve the highest possible resolution, the laser chip source must be oriented perpendicular to the line scan sensor and should be imaged onto the target. The expanded beam then converges in the orientation relating to the ranging. We derive the precise range from trigonometric back-calculation from the known distance to the termination, pixel sizes and transmitter-receiver separation distance. The angular sampling implies that the range sampling has a tangential range behavior, where pixels approaching the infinity pixel represent increasingly deep air

volumes. Apart from sampling the actual range, resolution additionally depends on diffraction limits of transmitter and receiver, and beam width in the plane of Fig. 4. The absolute optical cross-section is calculated from the known pixel footprint size and reflectance at the termination. Both in lidar and dark-field methods we can further verify optical cross sections through calibration with a size range of Teflon spheres dropped through the laser beam at different distances.

A CW Scheimpflug lidar arrangement yields several advantages over a conventional pulsed lidar system. The continuous radiation poses less eye-safety concerns and does not require high damage threshold transmitting optics. The instrumentation weight, size and cost can be brought down to few percent when comparing CW to pulsed lidars. Whereas pulsed lidar monitoring is generally pursued using cascade detectors such as Photo-Multiplier-Tubes (PMTs) or Avalanche-Photo-Diodes (APDs) limited to the spectral range 0.2–1.7 μm, CW lidars can be accomplished with Si, InGaAs or HgCdTe linear arrays within the range 0.2–12 μm.

In pulsed lidars, the repetition rate is constrained by the round trip time of the light. For example, monitoring 10 km range is limited to 15 kHz sample rate; thus the Nyquist frequency and highest resolvable modulation is 7.5 kHz. In comparison we have observed harmonic frequencies three times as high from common fruit flies. The major challenge associated with CW lidars is the background suppression. The main approaches to solve this problem are the use of high brightness lasers, small pixel height detectors, tailored filters, and lock-in methods with AC detection.

## 4. APPROACHES AND REASONS FOR BREAKING THE DIFFRACTION LIMIT

Since Ernst Karl Abbe presented his microscope work in 1873, it has been generally accepted that angular resolution in optical imaging is constrained to the wavelength divided by the numerical aperture. However, during recent decades this limitation has been circumvented through various approaches. In stimulated emission depletion (STED) fluorescence microscopy, the point spread function can be narrowed beyond the diffraction limit through the usage of a secondary toroidal depletion laser beam [23–25], whereby optical resolution is pushed to few tens of nanometers (A somewhat related improved resolution in the *spectral* domain is obtained in high-contrast Doppler-free transmission spectroscopy [26, 27], also relying on a non-linear response-saturation).

While the STED approach is based on a complicated laser scheme, other approaches, photo-activation localization microscopy (PALM) [28] and stochastic optical reconstruction microscopy (STORM) [29, 30], are based on sensitive cameras, single molecule detection and blinking molecules. In STORM, sparse dye molecules which randomly switch between fluorescing and dark states are imaged over time. Although each molecule gives rise to a point spread function broadened to the diffraction limit, through analyzing the ensemble of images over time, the center-of-mass of each dye molecule can be estimated to a much higher precision than Abbe's criterion would allow. In particular, we conclude from this, that the *angular* resolution can exceed the diffraction limit in a situation where *sparsely* distributed *blinking* particles appear.

Apart from astonishing close-up microscopic color images, the major scientific outcome of super resolution microscopy can be placed under the common category of co-location analysis. Here, particular interest is of the spatial co-occurrence and vicinity of differently labeled organelles and proteins in cellular biochemistry. Equivalently, turning to the case of the structure of the atmospheric fauna, there may not be a reason to pursue super resolution lidar for resolving the absolute position of the fauna constituents. Actually, most ground topography is varying on a spatial scale where conventional lidars can provide resolution, e.g., of the confinements due to preferred plants and similar [7]. However, when considering *in-situ* assessment of interaction kinetics and strength, insects, birds or bats appear separated by few centimeters or even appear in tandem flights [6].

Employing the method during field campaigns in Sweden we captured in the order of twenty thousand insects per cubic meter per night, providing large statistics for time-lag correlation [6] and co-location analysis. A close-up time range map of two simultaneous examples are shown in Fig. 5. The two insects here appear well resolved in distance but overlapping in time.

We will now explain how insects can be spatially resolved when flying very close to each other and while having their diffraction-limited distributions in the range domain strongly overlapping. In Fig. 6, we present a false color RGB composition time-range lidar map illustrating this, in a case with no overlap

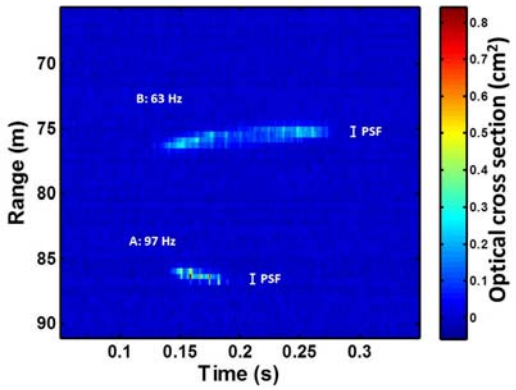


**Figure 5.** Our Scheimpflug lidar setup allows us to capture range-time lidar maps with spatial resolution in centimeters and temporal resolution in kHz. In this example, two individual insects are monitored simultaneously at 2 kHz sampling rate. The individual A actually corresponds to the data shown in Fig. 2(a); the frequency contents of individual A and B is likewise shown in Fig. 2(b). The figure shows a fraction of a larger range-time map covering 1800 meters and 5 seconds. Our method is not limited in sampling rate by the round-trip time of the light as in conventional lidars but by the average power of the laser.

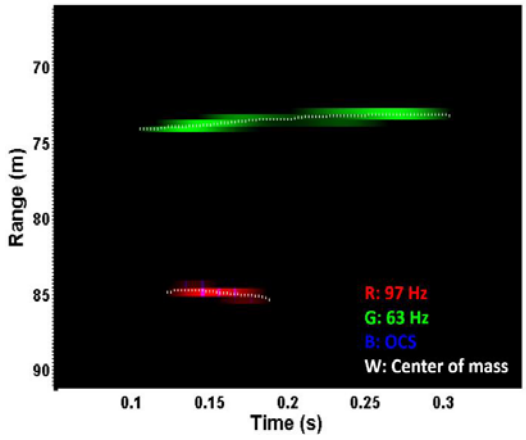


**Figure 6.** When we apply the modulation signatures from Fig. 2(b) as sliding filters, we can produce species specific color coded range-time maps. Because of the sparse nature of the atmospheric fauna the center-of-mass of the echo energy can be estimated at a sub-pixel and sub-diffraction level. This can shine new light on interacting atmospheric fauna constituents.

between the point-spread-function (PSF). After subtracting electronic and optical background as well as the static atmospheric backscatter, the back-scatter signal is calibrated to absolute cross section. We apply sliding temporal matched filters with transmittance identical to the modulation power spectra presented in Fig. 2(b), pertaining to these particular types of insects. In other words, each element in the time-range map in Fig. 5 is projected into the two base modulation spectra in Fig. 2(b), whereupon two values are obtained for every time-range element. If the element and time adjacent elements within the sliding windowmatch the modulation of either of the modulation spectra in Fig. 2(b), the respective projection will be large.

The insects are thus classified by their full modulation spectra as in, e.g., [11]. In practical usage the fundamental frequency of the same species/sex is expected to vary with the ambient temperature, which must then be compensated for. Insects are also known to have a large natural spread of absolute cross-sections within species [4]; however, the relative strength between harmonics or modulation spectral shape is believed to vary less. The filters are Gaussian and with 38 ms FWHM, and are defined in

100 linearly distributed frequency points between 10 Hz and 600 Hz. In the red channel the original backscatter signal in Fig. 5 is filtered by the individual A and in the green channel it is filtered by individual B. Apart from projection on the two temporal filters in Fig. 2(b) and linear stretching to the dynamic of the RGB image, no further digital enhancement is applied. There is no significant cross-talk in this case — thus no contribution of the 97 Hz individual A on the green channel nor any contribution of the 63 Hz individual B to the red channel. Thus, the method works equivalently for two individuals overlapping beyond the diffraction limit. The presented lidar data in Fig. 5 originate from a campaign where insect interactions are believed to be much rarer than the case of the dark field data presented in Fig. 1.

On the output from the projection of the two filters we can apply a centre-of-mass to estimate range beyond pixel and diffraction limits, in analogy with centroid localization in super resolution microscopy [28]. The respective centre-of-mass is plotted as white dotted lines. These range values are obtained by Scheimpflug lidar where the retrieved incidence angle of the light is translated to range. As such the range resolution is normally limited by the angular resolution, but here it is unrestricted by the diffraction limit due to the sparse and blinking property of the atmospheric insects. From the range stability of the lines, it is understood that range is estimated below pixel and diffraction limit with the given time window settings.

## 5. DISCUSSION

In conclusion, the presented super resolution lidar methods promise quantitative *in-situ* mapping of interaction strengths and kinetics between prey, predators, sexes or competitors. This is currently unavailable information, which might prove most crucial for understanding the mechanisms of ecosystems and for the managing a sustainable and healthy environment. Interaction strength are assessed via time-lag correlation analysis as in [6]. This implies that the likelihood of observing a certain species or sex in a confined air volume is altered if the very same air volume was occupied by another species or sex the moments before. The lidar examples presented in this study were recorded during night time in a scenario, where less insect interaction is expected in respect to Fig. 1. Accordingly, two spatially overlapping individuals could not be found in the given dataset although the method would work equivalently in such cases. We have later on refined the background rejection filters and have been able to record lidar signals during day time.

Apart from co-occurrence in time and space, indications of interaction can additionally be verified by observation of the same flight heading direction as in Fig. 1 using quadrant detectors. By employing a sensor with two or more rows of pixels,or a dual-chip laser source the consecutive interception can be retrieved and additional verification of interaction can be confirmed.

In respect to super resolution microscopy methods, a fundamental difference is that in our case two close lying insects with identical modulation spectra cannot be differentiated. In this study we merely investigate the modulation power spectrum and not the phase which could address this concern. This discrepancy from super resolution microscopy would also apply to a variety of our method, where multi-band lidars with spectral discrimination rather than modulation discrimination is pursued.

There are a few constraints and limitations associated with the presented method. Frequency analysis requires a time window; thus the temporal identification in Fig. 6 is broadened in respect to the original data in Fig. 5. This inherent property of the Fourier transform is also illustrated in Fig. 2. Additionally, the recording of wing beats require a certain beam width, the lateral position of insect in the beam induces uncertainty in the range estimation. This could be circumvented in a number of ways, e.g. by adding an additional receiver. In respect to back-ground rejection, band-pass filtering of convergent light constitutes a well-known problem.

As for the case of dyes binding to diverse organelles in super-resolution fluorescence microscopy [23, 30], remotely detected insects can be used for indirect sensing of single molecules through their superior olfactory capabilities [31]. Thus, entomological lidar can be used as a tool even for researchers outside entomology searching for lidar application for ultra-low concentration of trace gases.This approach has been explored since almost a decade for land-mine detection. In these studies bees are trained to correlate the smell of evaporating explosives with nutrition, and when deployed at a mine field the bee abundance measured with lidar can be correlated with mine sites [32, 33].

The presented kHz lidar scheme advances the portability and reduces cost in respect to previous systems. The method can be further developed, e.g., with multiple bands or polarization modes by time-multiplexing. Such improvements increase specificity for species, sexes and age groups and can yield additional information regarding, e.g., melanization, body fur, payloads such as blood-meals and pollen, or details on wing thickness and refractive index as discussed above. A major challenge is to formulate table values for insect cross sections. This problem is closely related to estimating the interception angle with the lidar. The challenge is addressed in [16] and could potentially reduce the uncertainty spread in projected cross section and also provide information on insect flux in the landscape at the same time.

The applications, opportunities and possible experiments of entomological lidar are to great extent outlined in recent literature regarding radar entomology [4] mainly with differences in technical and performance. In particular we envision applications for evaluating and managing ecosystems in the areas of ecological and sustainable food production and forestry, for the understanding of disease vector and pest dispersal, and for assessing biodiversity from a conservation perspective. Mapping out interaction strengths and kinetics between species or genders is of interest in fundamental research in ecology. Interaction strengths can be recorded for identifying matched predators in ecological bio-control of pests, or for predicting consequences of invasive species with a climate change perspective, other research groups pursue aerial insect interaction from a flight mechanics and bio-inspiration perspective [9]. The lidar method is compatible with fluorescence lidar for powder marked insects [7] if an RGB sensor is employed. This could allow for assessment of absolute population sizes, life-times, landscape dispersal rates, or for comparative studies of the behavior of residents and migrants.

## ACKNOWLEDGMENT

We thank Erich Rohwer, Hubertus V. Bergmann, Pieter Neethling, Gerhard Louwrens, Lawrence Ashworth, Nanike Esterhuizen and John Terreblanche for the hospitality and assistance during work at Stellenbosch University. We thank Susanne Åkesson, Maren Wellenreuther, and Anna Runemark for continuous support, and interdisciplinary collaboration with CAnMove, Department of Biology, Lund University. We thank the International Science Program, Uppsala, Sweden for continuing support of physics in Africa.

## REFERENCES

1. Potts, S. G., J. C. Biesmeijer, C. Kremen, P. Neumann, O. Schweiger, and W. E. Kunin, "Global pollinator declines: trends, impacts and drivers," *Trends Ecol. Evol.*, Vol. 25, 345-353, doi:10.1016/j.tree.2010.01.007, 2010.
2. Pasquet, R. S., A. Peltier, M. B. Hufford, E. Oudin, J. Saulnier, L. Paul, J. T. Knudsen, H. R. Herren, and P. Gepts, "Long-distance pollen flow assessment through evaluation of pollinator foraging range suggests transgene escape distances," *PNAS*, Vol. 105, 13456–13461, doi:10.1073/pnas.0806040105, 2008.
3. Ovaskainen, O., A. D. Smith, J. L. Osborne, D. R. Reynolds, N. L. Carreck, A. P. Martin, K. Niitepõld, and I. Hanski, "Tracking butterfly movements with harmonic radar reveals an effect of population age on movement distance," *PNAS*, Vol. 105, 19090–19095, doi:10.1073/pnas.0802066105, 2008.
4. Drake, V. A. and D. R. Reynolds, *Radar Entomology: Observing Insect Flight and Migration*, CABI, Wallingford, Oxfordshire, Boston, MA, 2012.
5. Brydegaard, M., P. Samuelsson, M. W. Kudenov, and S. Svanberg, "On the exploitation of mid-infrared iridescence of plumage for remote classification of nocturnal migrating birds," *Appl. Spectr. (including front page feature)*, Vol. 67, 477–490, 2013.
6. Runemark, A., M. Wellenreuther, H. Jayaweera, S. Svanberg, and M. Brydegaard, "Rare events in remote dark field spectroscopy: an ecological case study of insects," *IEEE JSTQE*, Vol. 18, 1573–1582, doi:10.1109/jstqe.2012.2184528, 2012.

7. Guan, Z., M. Brydegaard, P. Lundin, M. Wellenreuther, A. Runemark, E. Svensson, and S. Svanberg, "Insect monitoring with fluorescence lidar techniques: field experiments," *Appl. Opt.*, Vol. 49, 1–11, 2010.
8. Mei, L., Z. G. Guan, H. J. L. J. Zhou, Z. R. Zhu, J. A. Cheng, F. J. Chen, Löfstedt, C., S. Svanberg, and G. Somesfalean, "Agricultural pest monitoring using fluorescence lidar techniques," *Appl. Phys. B*, Vol. 106, 733–740, doi:10.1007/s00340-011-4785-8, 2011.
9. Combes, S. A., D. E. Rundle, J. M. Iwasaki, and J. D. Crall, "Linking biomechanics and ecology through predator-prey interactions: Flight performance of dragonflies and their prey," *J. Exp. Biol.*, Vol. 215, 903–913, 2012.
10. Antoci, V., G. Handler, T. L. Campante, A. O. Thygesen, A. Moya, T. Kallinger, D. Stello, A. Grigahcène, H. Kjeldsen, T. R. Bedding, T. Lüftinger, J. Christensen-Dalsgaard, G. Catanzaro, A. Frasca, P. De Cat, K. Uytterhoeven, H. Bruntt, G. Houdek, D. W. Kurtz, and P. Lenz, "The excitation of solar-like oscillations in a $\delta$Sct star by efficient envelope convection," *Nature*, Vol. 477, 570–573, doi:10.1038/nature10389, 2011.
11. Moore, A. and R. H. Miller, "Automated identification of optically sensed aphid (*Homoptera: Aphidae*) wingbeat waveforms," *Ann. Entomol. Soc. Am.*, Vol. 95, 1–8, 2002.
12. Batista, G. E., E. J. Keogh, A. Mafra-Neto, and E. Rowton, *Secondary "SIGKDD demo: Sensors and software to allow computational entomology, an emerging application of data mining,"* 761–764, ACM, San Diego, California, USA, 2011.
13. Svensson, E. I., F. Eroukhmanoff, K. Karlsson, A. Runemark, and A. Brodin, "A role for learning in population divergence of mate preferences," *Evolution*, Vol. 64, 3101–3113, 2010.
14. Mayagaya, V. S., K. Michel, M. Q. Benedict, G. F. Killeen, R. A. Wirtz, H. M. Ferguson, and F. E. Dowell, "Non-destructive determination of age and species of *Anopheles gambiaes.l.* using Near-infrared spectroscopy," *Am. J. Trop. Med. Hyg.*, Vol. 81, 622–630, doi:10.4269/ajtmh.2009.09-0192, 2009.
15. Peiris, K. H., B. S. Drolet, L. W. Cohnstaedt, and F. E. Dowell, "Infrared absorption characteristics of *culicoides sonorensis* in relation to insect age," *American Journal of Agricultural Science and Technology*, Vol. 2, 49–61, 2014.
16. Török, S., *Kilohertz Electro-optics for Remote Sensing of Insect Dispersal*, Master thesis, Lund University, 2013.
17. Althausen, D., D. Muller, A. Ansmann, U. Wandinger, H. Hube, E. Clauder, and S. Zorner, "Scanning 6-wavelength 11-channel aerosol lidar," *J. Atmospheric, and Oceanic Tech.*, Vol. 17, 1469, 2000.
18. Jonsson, P., M. Elmqvist, O. Gustafsson, F. Kullander, R. Persson, G. Olofsson, T. Tjarnhage, O. Farsund, T. V. Haavardsholm, and G. Rustad, "Evaluation of biological aerosol stand-off detection at a field trial," *Proc. of SPIE*, 74840I-74814, 2009.
19. Shevtsova, E., C. Hansson, D. H. Janzen, and J. Kjaerandsen, "Stable structural color patterns displayed on transparent insect wings," *PNAS*, Vol. 108, 668–673, doi:10.1073/pnas.1017393108, 2011.
20. Brydegaard, M., "Advantages of shortwave infrared LIDAR entomology," *Imaging and Applied Optics*, LW2D.6 Optical Society of America, 2014.
21. Yin, H., L. Shi, J. Sha, Y. Li, Y. Qin, B. Dong, S. Meyer, X. Liu, L. Zhao, and J. Zi, "Iridescence in the neck feathers of domestic pigeons," *Phys. Rev. E*, Vol. 74, 051916, doi:10.1103/PhysRevE.74.051916, 2006.
22. Blais, F., "Review of 20 years of range sensor development," *J. Electron. Imaging*, Vol. 13, 231–243, doi:10.1117/1.1631921, 2004.
23. Hell, S. W., "Far-field optical nanoscopy," *Science*, Vol. 316, 1153–1158, doi:10.1126/science.1137395, 2007.
24. Klar, T. A. and S. W. Hell, "Subdiffraction resolution in far-field fluorescence microscopy," *Opt. Lett.*, Vol. 24, 954–956, 1999.

25. Hell, S. W. and J. Wichmann, "Breaking the diffraction resolution limit by stimulated emission: Stimulated-emission-depletion fluorescence microscopy," *Opt. Lett.*, Vol. 19, 780–782, doi:10.1364/OL.19.000780, 1994.
26. Svanberg, S., G. Y. Yan, T. P. Duffey, and A. L. Schawlow, "High-contrast Doppler-free transmission spectroscopy," *Opt. Lett.*, Vol. 11, 138–140, doi:10.1364/OL.11.000138, 1986.
27. Svanberg, S., G. Y. Yan, T. P. Duffey, W. M. Du, T. W. Hänsch, and A. L. Schawlow, "Saturation spectroscopy for optically thick atomic samples," *J. Opt. Soc. Am. B*, Vol. 4, 462–469, doi:10.1364/JOSAB.4.000462, 1987.
28. Betzig, E., G. H. Patterson, R. Sougrat, O. W. Lindwasser, S. Olenych, J. S. Bonifacino, M. W. Davidson, J. Lippincott-Schwartz, and H. F. Hess, "Imaging intracellular fluorescent proteins at nanometer resolution," *Science*, Vol. 313, 1642–1645, doi:10.1126/science.1127344, 2006.
29. Rust, M. J., M. Bates, and X. Zhuang, "Sub-diffraction-limit imaging by stochastic optical reconstruction microscopy (STORM)," *Nat. Methods*, Vol. 3, 793–795, doi:10.1038/nmeth929, 2006.
30. Huang, B., M. Bates, and X. Zhuang, "Super-resolution fluorescence microscopy," *Ann. Rev. Biochem.*, Vol. 78, 993–1016, doi:doi:10.1146/annurev.biochem.77.061906.092014, 2009.
31. Kaissling, K.-E. and E. Priesner, "Die Riechschwelle des Seidenspinners," *Naturwissenschaften*, Vol. 57, 23–28, doi:10.1007/BF00593550, 1970.
32. Shaw, J. A., N. L. Seldomridge, D. L. Dunkle, P. W. Nugent, and L. H. Spangler, "Polarization lidar measurements of honey bees in flight for locating land mines," *Opt. Expr.*, Vol. 13, 5853–5863, 2005.
33. Carlsten, E. S., G. R. Wicks, K. S. Repasky, J. L. Carlsten, J. J. Bromenshenk, and C. B. Henderson, "Field demonstration of a scanning lidar and detection algorithm for spatially mapping honeybees for biological detection of land mines," *Appl. Opt.*, Vol. 50, 2112–2123, 2011.